Electronic Supplementary Information

Hysteresis in the Ground and Excited Spin State Up to 10 T of a $[Mn^{III}_6Mn^{III}]^{3+}$ Triplesalen Single-Molecule Magnet

Veronika Hoeke,[a] Klaus Gieb,[b] Paul Müller,[b] Liviu Ungur,[c] Liviu F. Chibotaru,[c] Maik Heidemeier,[a] Erich Krickemeyer,[a] Anja Stammler,[a] Hartmut Bögge,[a] Christian Schröder,[d] Jürgen Schnack,[e] Thorsten Glaser*[a]

[a] Fakultät für Chemie, Universität Bielefeld, D-33615 Bielefeld, Germany. E-mail: thorsten.glaser@uni-bielefeld.de

[b] Physikalisches Institut III, Universität Erlangen-Nürnberg, D-91058 Erlangen, Germany

[c] Division of Quantum and Physical Chemistry, Katholieke Universiteit Leuven, B-3001 Heverlee, Belgium

[d] Fachbereich Ingenieurwissenschaften und Mathematik, Fachhochschule Bielefeld, D-33602 Bielefeld, Germany

[e] Fakultät für Physik, Universität Bielefeld, D-33615 Bielefeld, Germany

Fig. S1. ORTEP plots of the two independent fragments ((a) and (b)) of **[$Mn^{III}_6Mn^{III}$]$^{3+}$** molecules in the asymmetric unit in crystals of **1** with the numbering scheme used. Thermal ellipsoids are drawn at the 50 % probability level; hydrogen atoms are omitted for clarity.

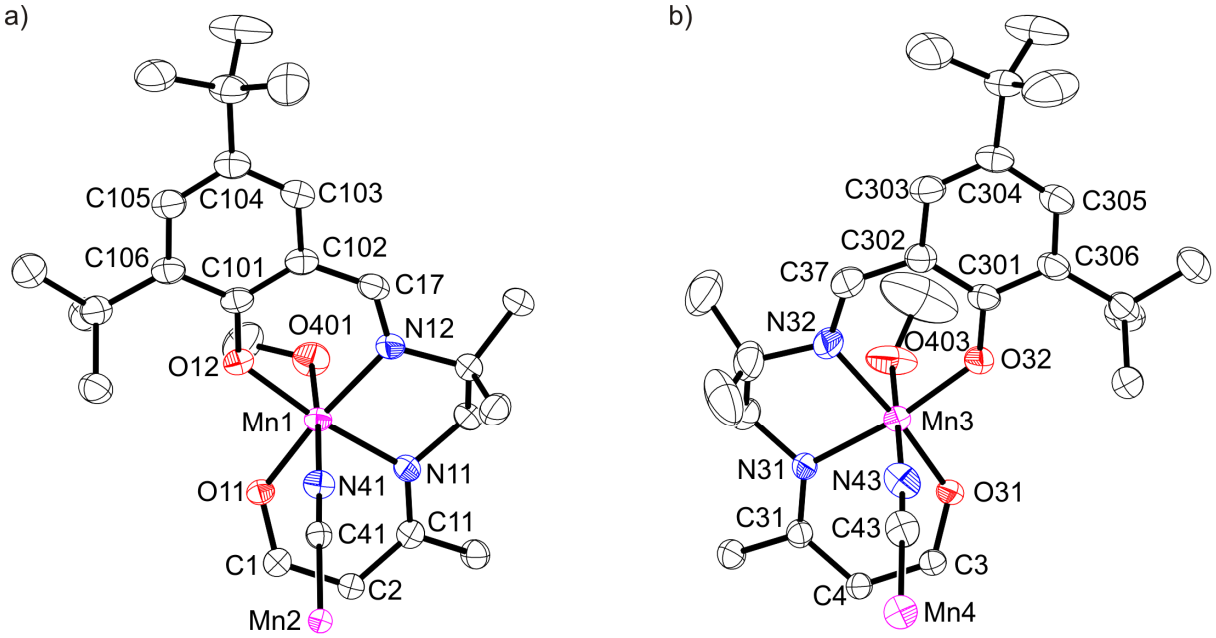

Fig. S2. Structure of (A) the calculated $[Mn^{III}(C{\equiv}N\text{-}Mn^{III})_6]^{15+}$ fragment in approximations A and B, and (B) the calculated $[Mn^{III}(CN)_6]^{3-}$ fragment in approximation C.

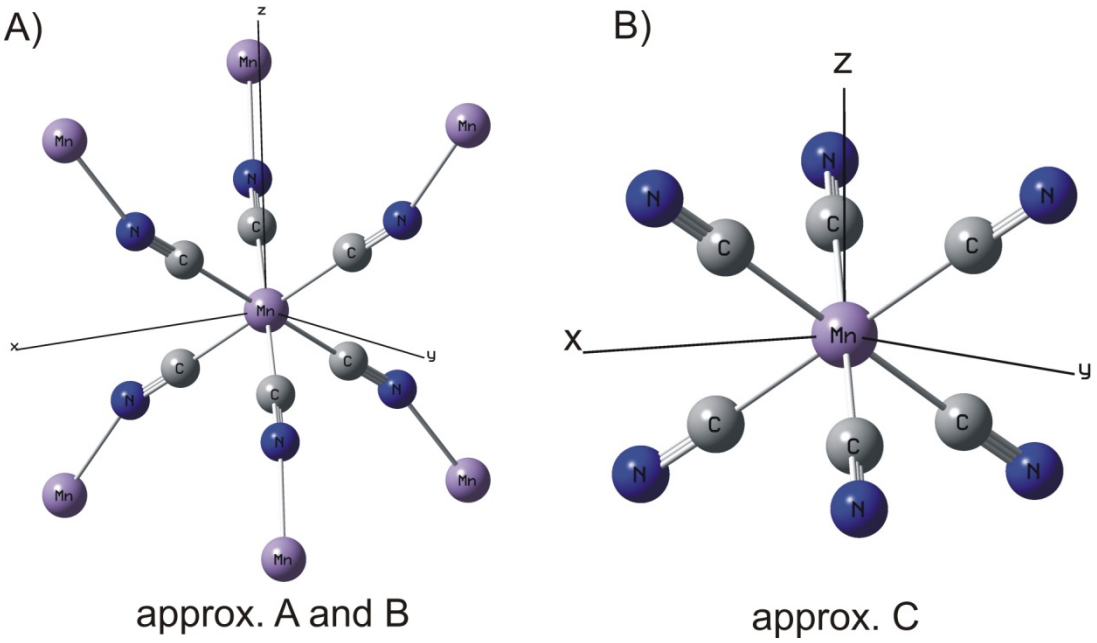

Fig. S3. Structure of the calculated $[\{(L)(Mn^{III}(H_2O))_3\}_2\{Mn^{III}(CN)_6\}]^{3+}$ fragment in approximation D. The fragment corresponds to the complete trication $\mathbf{[Mn^{III}_6Mn^{III}]^{3+}}$ except for some of the substituents of the ligand backbone, *e.g.* the *t*-Bu groups, that have been replaced by hydrogen atoms in the *ab initio* calculation.

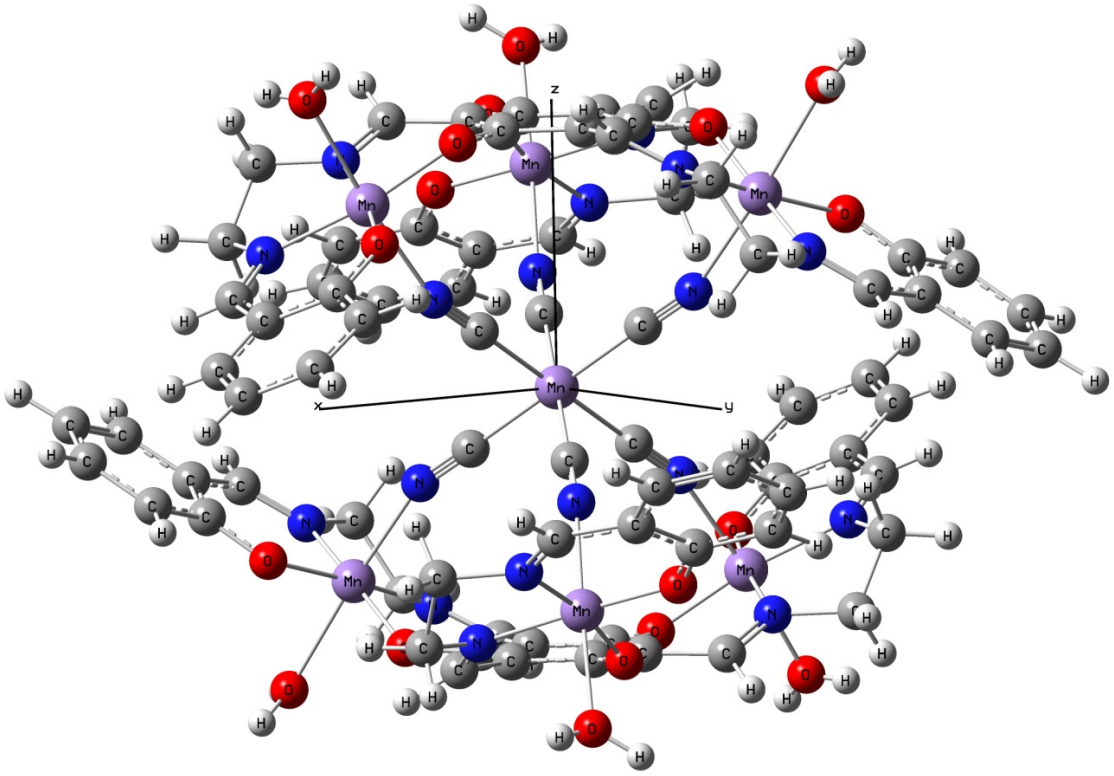

Table S1. Selected Interatomic Distances [Å] and Angles [deg] for **1**.

Mn(1)-O(11)	1.890(2)
Mn(1)-O(12)	1.887(2)
Mn(1)-N(11)	1.983(3)
Mn(1)-N(12)	1.982(3)
Mn(1)-N(41)	2.189(3)
Mn(1)-O(401)	2.287(3)
O(11)-C(1)	1.310(4)
O(12)-C(101)	1.316(4)
N(11)-C(11)	1.297(4)
N(12)-C(17)	1.292(4)
C(1)-C(2)	1.423(4)
C(1)-C(2)#1	1.422(4)
C(2)-C(11)	1.454(4)
C(17)-C(102)	1.428(5)
C(101)-C(102)	1.413(5)
C(101)-C(106)	1.429(5)
C(102)-C(103)	1.416(5)
C(103)-C(104)	1.365(5)
C(104)-C(105)	1.402(5)
C(105)-C(106)	1.388(5)
Mn(1)-Mn(1)#1	6.8152(10)
Mn(1)-Mn(2)	5.2442(6)
Mn(2)-C(41)	1.980(3)
N(41)-C(41)	1.149(4)
Mn(3)-O(31)	1.882(2)
Mn(3)-O(32)	1.885(2)
Mn(3)-N(31)	1.980(3)
Mn(3)-N(32)	1.974(3)
Mn(3)-N(43)	2.190(3)
Mn(3)-O(403)	2.332(3)
O(31)-C(3)	1.312(4)
O(32)-C(301)	1.318(4)
N(31)-C(31)	1.324(4)
N(32)-C(37)	1.296(5)
C(3)-C(4)	1.411(4)
C(3)-C(4)#1	1.426(4)
C(4)-C(31)	1.452(4)
C(37)-C(302)	1.427(5)
C(301)-C(302)	1.421(5)
C(301)-C(306)	1.420(5)
C(302)-C(303)	1.417(5)
C(303)-C(304)	1.368(5)
C(304)-C(305)	1.412(5)
C(305)-C(306)	1.384(5)
Mn(3)-Mn(3)#1	6.7770(11)
Mn(3)-Mn(4)	5.2628(6)
Mn(4)-C(43)	1.990(4)
N(43)-C(43)	1.149(5)
O(12)-Mn(1)-O(11)	95.85(9)
O(12)-Mn(1)-N(12)	92.14(11)
O(11)-Mn(1)-N(12)	170.18(11)
O(12)-Mn(1)-N(11)	172.72(10)
O(11)-Mn(1)-N(11)	88.86(10)
N(12)-Mn(1)-N(11)	82.65(11)
O(12)-Mn(1)-N(41)	93.10(10)
O(11)-Mn(1)-N(41)	89.62(10)
N(12)-Mn(1)-N(41)	95.67(11)
N(11)-Mn(1)-N(41)	92.47(11)
O(12)-Mn(1)-O(401)	87.42(10)
O(11)-Mn(1)-O(401)	85.65(10)
N(12)-Mn(1)-O(401)	89.02(11)
N(11)-Mn(1)-O(401)	87.42(11)
N(41)-Mn(1)-O(401)	175.26(11)
Mn(2)-Mn(1)-Mn(1)#1	49.475(5)
C(1)-O(11)-Mn(1)	124.19(19)
C(101)-O(12)-Mn(1)	130.7(2)
C(41)#1-Mn(2)-C(41)	91.88(12)
C(41)-N(41)-Mn(1)	160.0(2)
N(41)-C(41)-Mn(2)	178.6(3)
O(31)-Mn(3)-O(32)	95.93(10)
O(31)-Mn(3)-N(32)	168.68(13)
O(32)-Mn(3)-N(32)	92.06(12)
O(31)-Mn(3)-N(31)	89.35(11)
O(32)-Mn(3)-N(31)	171.24(11)
N(32)-Mn(3)-N(31)	81.79(13)
O(31)-Mn(3)-N(43)	90.52(11)
O(32)-Mn(3)-N(43)	94.39(11)
N(32)-Mn(3)-N(43)	96.87(14)
N(31)-Mn(3)-N(43)	92.55(12)
O(31)-Mn(3)-O(403)	86.19(11)
O(32)-Mn(3)-O(403)	88.15(11)
N(32)-Mn(3)-O(403)	86.06(15)
N(31)-Mn(3)-O(403)	85.22(12)
N(43)-Mn(3)-O(403)	176.04(12)
Mn(4)-Mn(3)-Mn(3)#1	49.920(5)
C(3)-O(31)-Mn(3)	123.57(19)
C(301)-O(32)-Mn(3)	131.1(2)
C(43)#1-Mn(4)-C(43)	90.65(14)
C(43)-N(43)-Mn(3)	161.7(3)
N(43)-C(43)-Mn(4)	178.9(4)

Symmetry transformations used to generate equivalent atoms:
#1 -y+1,x-y+1,z

Mn6Mn_c_axis.avi:
Title: Classical spin dynamics simulation of **[$Mn^{III}_6Mn^{III}$]$^{3+}$** at T = 0 K.
Video Legend: Starting from the ground state in which the spins (red arrows) are almost aligned to their local anisotropy axes (yellow sticks), a magnetic field ramp (blue arrow) is applied parallel to the molecular S_6 axis. At about 5 T, two spins flip from the opposite direction into the direction of the magnetic field. Due to the strong anisotropies even at high magnetic fields, the spins are not fully aligned to the external field.

Mn6Mn_c_axis_slow_motion.avi:
Title: Slow motion of the spin flip process shown in movie Mn6Mn_c_axis.avi.
Video Legend: Due to the weak exchange interactions among the spins, the reorientation of the two flipping spins causes the remaining spins to precess.

Mn6Mn_40deg.avi:
Title: Classical spin dynamics simulation of **[$Mn^{III}_6Mn^{III}$]$^{3+}$** at T = 0 K.
Video Legend: Starting from the ground state in which the spins (red arrows) are almost aligned to their local anisotropy axes (yellow sticks), a magnetic field ramp (blue arrow) is applied at 40° to the molecular S_6 axis, *i.e.* parallel to two of the anisotropy axis of the molecule. At about 7.5 T, two spins flip from the opposite direction into the direction of the magnetic field. Due to the strong anisotropies even at high magnetic fields, four spins are not fully aligned to the external field.

Mn6Mn_40deg_slow_motion.avi:
Title: Slow motion of the spin flip process shown in movie Mn6Mn_40deg.avi.
Video Legend: Due to the weak exchange interactions among the spins, the reorientation of the two flipping spins causes the remaining spins to precess.